



Research paper

Improved anticancer and antiparasitic activity of new lawsone Mannich bases



Katharina Mahal^{a,1}, Aamir Ahmad^{b,1}, Florian Schmitt^a, Julia Lockhauserbäumer^c, Kathrin Starz^c, Rohan Pradhan^d, Subhash Padhye^d, Fazlul H. Sarkar^b, Waleed S. Koko^{e,f}, Rainer Schobert^a, Klaus Ersfeld^c, Bernhard Biersack^{a,*}

^a Organic Chemistry Laboratory, University of Bayreuth, Universitaetsstrasse 30, 95440 Bayreuth, Germany

^b Karmanos Cancer Institute, Dept. of Pathology, Wayne State University, Detroit 48201, USA

^c Laboratory of Molecular Parasitology, Department of Genetics, University of Bayreuth, 95440 Bayreuth, Germany

^d Department of Chemistry, Abeda Inamdar Senior College, Pune 411001, India

^e Department of Microbiology and Parasitology, Medicinal and Aromatic Plants Research Institute, National Centre for Research, Khartoum, Sudan

^f College of Science and Arts (Ar Rass), Qassim University, Buraidah, Saudi Arabia

ARTICLE INFO

Article history:

Received 10 September 2016

Received in revised form

1 November 2016

Accepted 21 November 2016

Available online 22 November 2016

Keywords:

Lawsone

Mannich base

Anticancer drugs

Antiparasitic drugs

ABSTRACT

Substituted lawsone Mannich bases **2a–e**, **3a–e** and **4a–e** were prepared and tested for their biological activities. The new fatty alkyl substituted compounds **2a–c** exhibited strong and selective growth inhibitory activities in the low one-digit micromolar and sub-micromolar range against a panel of human cancer cell lines associated with ROS formation. In addition, compounds **2a–c** revealed sub-micromolar anti-trypanosomal activities against parasitic *Trypanosoma brucei brucei* cells via deformation of the microtubule cytoskeleton. The *N*-hexadecyl compound **2c** was also highly active against locally isolated *Entamoeba histolytica* parasite samples exceeding the activity of metronidazole.

© 2016 Elsevier Masson SAS. All rights reserved.

1. Introduction

Naphthoquinones feature a large group of secondary plant and lichen metabolites with a broad range of properties including antioxidant, anti-inflammatory, anticancer, antibacterial, and trypanocidal activities [1–5]. Lawsone, 2-hydroxy-1,4-naphthoquinone (Fig. 1), is a constituent of the Henna plant (*Lawsonia inermis*) applied mainly for the treatment of skin diseases in Ayurveda and Unani medicine in South Asia [3–7]. Its biological properties are only fragmentarily explored, and in contrast to other natural naphthoquinones such as plumbagin and juglone, lawsone only showed weak toxicity both to hepatocytes and to various tumor cell lines [8–12]. Lawsone is a potentially useful starting material for the preparation of other *p*-quinones with proven or conceivable bioactivity such as atovaquone or lapachol [3,4]. The readiness with which naphthoquinone derivatives undergo redox

reactions and chelation of metal ions is presumably responsible for the greater part of their biological activities [4]. Ferrocenic aminohydroxynaphthoquinones derived from lawsone were reported to inhibit the growth of *Toxoplasma gondii* parasites [13]. *O*-Allyl and *C*-allyl lawsone derivatives and the naphthofuranquinone cyclization products of the latter showed distinct activity against *Trypanosoma cruzi* parasites [14,15]. Some phenyl ethers of lawsone exhibited potent activity against *Trypanosoma brucei rhodesiense* and *Leishmania donovani* [16]. Fatty alkyl substituted lawsones revealed trypanocidal activity against the infective blood stream form of *T. cruzi* [17]. Pronounced anti-plasmodial activity against *Plasmodium falciparum* was observed for phenylsulfanylmethyl naphthoquinones based on lawsone [18]. A series of anticancer active 3-aminomethyl-naphthoquinones readily obtained from lawsone via a one-pot Mannich reaction was disclosed recently (e.g., **1**, Fig. 1) [19–22]. We now refined the structural motif of **1** by elongation of the *N*-alkyl side chain since long-chained alkyl residues were frequently found to confer enhanced bioactivity [23]. In addition, we explored the feasibility of other molecular fragments such as the vanillyl moiety that occurs in many bioactive natural

* Corresponding author.

E-mail address: bernhard.biersack@yahoo.com (B. Biersack).

¹ Both authors contributed equally to this work.

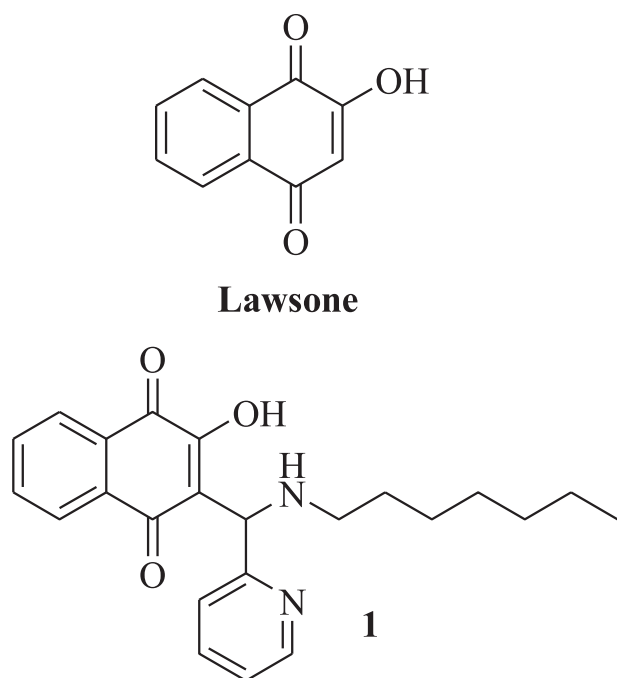


Fig. 1. Lawsone and its anticancer active derivative **1**.

products (e.g., in curcumin and ferulic acid), and the isosteric 3,4-difluorophenyl moiety. It was recently disclosed that certain naphthoquinone derivatives possessed multi-targeting properties including potent anticancer, anti-Alzheimer's and anti-trypanosomal activities [24–26]. Thus, the anticancer and anti-parasitic activities of the new lawsone derivatives were evaluated

on a panel of human cancer cell lines, in parasitic *Trypanosoma brucei brucei* cells that differ strongly from *T. cruzi* parasites concerning cell surface structure, and in *Entamoeba histolytica* samples isolated from amoebiasis patients.

2. Results and discussion

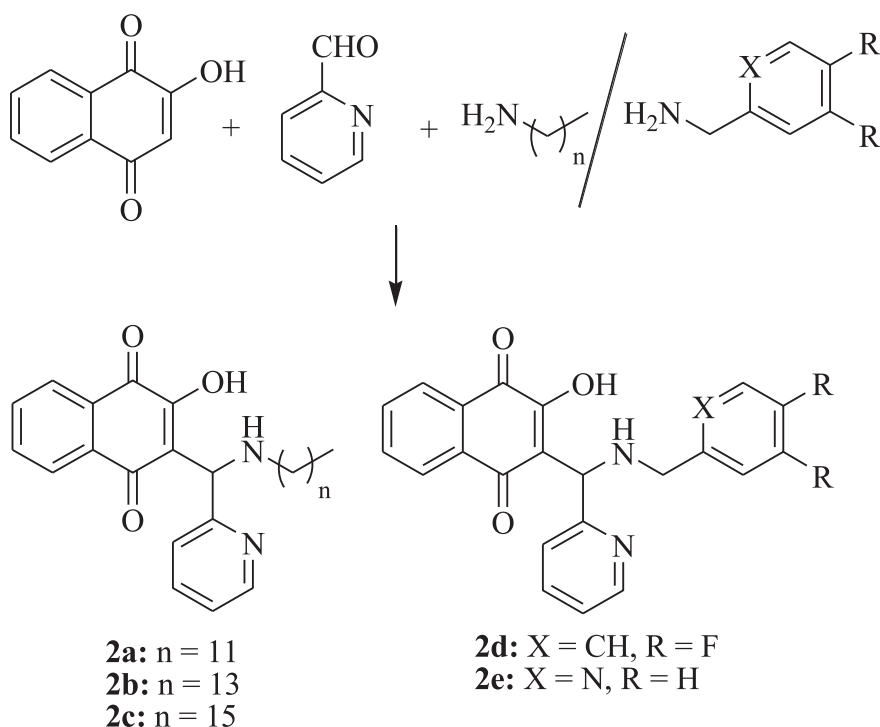
2.1. Chemistry

The Mannich bases **2a–e** were prepared via Mannich reaction of lawsone, 2-pyridylcarboxaldehyde and the corresponding amine, in detail, dodecyl amine for **2a**, tetradecyl amine for **2b**, hexadecyl amine for **2c**, 3,4-difluorobenzylamine for **2d**, and 2-pyridylmethylamine for **2e** [27] in moderate to good yields (Scheme 1). The desired products precipitated as racemic orange-red solids from the reaction mixture after stirring in EtOH for a few hours.

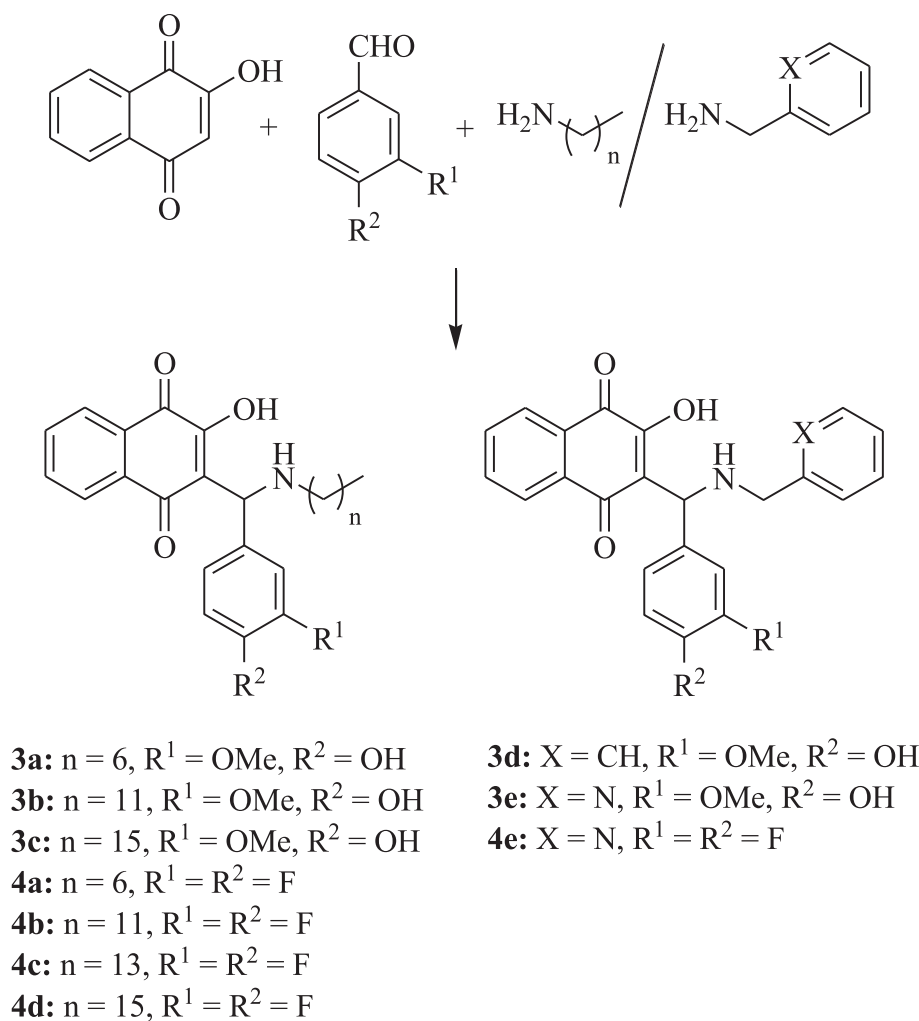
In addition, closely related vanillyl and 3,4-difluorophenyl derivatives **3a–e** and **4a–e** were prepared (Scheme 2). Analogously to the synthesis of compounds **2a–e**, the Mannich reaction of lawsone with vanillin and the corresponding primary amine in EtOH gave the Mannich bases **3a–e** as orange-red solids. In addition, reaction of lawsone with 3,4-difluorobenzaldehyde and various primary amines led to compounds **4a–e** (orange-red solids). These target compounds were obtained in moderate to high yields.

2.2. Anticancer activity

Compounds **2a–e**, **3a–e** and **4a–e** were initially tested for their growth inhibitory activity against human triple-negative MDA-MB-231 breast carcinoma, gemcitabine-sensitive BxPC-3 pancreas carcinoma, and androgen-refractory PC-3 prostate cancer cells and compared with the activity of **1** (Fig. 2, Figs. S1–S6, Supporting information). Compound **2c** with a long aliphatic hexadecyl side-



Scheme 1. Reagents and conditions: EtOH, r.t., 5 h, 44–71%.



Scheme 2. Reagents and conditions: EtOH, r.t., 5 h, 39–93%.

chain exhibited the highest activity of this series in these three cancer cell lines ($IC_{50} = 1.1 \pm 0.09 \mu\text{M}$ for MDA-MB-231, $0.82 \pm 0.04 \mu\text{M}$ for BxPC-3, and $0.67 \pm 0.04 \mu\text{M}$ for PC-3 cells) and revealed significantly higher growth inhibitory activity than the known compound **1** at low concentrations ($1 \mu\text{M}$) (Fig. 2, Figs. S1 and S2). **2c** was particularly active against the PC-3 prostate cancer cells. In addition, compound **2c** was virtually inactive against non-malignant human MCF-10A breast epithelial cells at doses as high as $50 \mu\text{M}$ (Fig. 3). Thus, compound **2c** exhibited distinct tumor selectivity.

The fatty alkyl vanillyl compounds **3a–c** exhibited a similar activity pattern with the *N*-hexadecyl derivative **3c** as the most active compound against these cancer cells and activities comparable with **2a** and **2b** while the *N*-heptyl derivative **3a** was virtually inactive at concentrations above $25 \mu\text{M}$ (Fig. 2, Fig. S3). The benzyl- and 2-pyridyl derivatives **3d** and **3e** showed no activity below $25 \mu\text{M}$ either (Fig. S4). The 3,4-difluorobenzyl analogs **4a–e** were the least active compounds and only revealed growth inhibitory activity at concentrations above $10–25 \mu\text{M}$ (Figs. S5 and S6). In addition, the influence of the length of the alkyl chains of compounds **4a–d** on the growth inhibitory activity of the compounds depended on the cell line. While in the PC-3 cells longer alkyl chains led to increased activities (**4c**, **4d**), in the BxPC-3 cells *N*-

dodecyl derivative **4b** was most active. Again, the heterocyclic 2-pyridyl-substituted compound **4e** showed no activity below $25 \mu\text{M}$.

Next, the compounds **1**, **2a–e** and **3c** were tested for their antiproliferative activity in additional four different metastatic and/or drug-resistant human cancer cell lines 518A2 melanoma, HCT-116 colon carcinoma, KB-V1(Vbl) cervix carcinoma, and Panc-1 pancreatic carcinoma (Table 1). Indeed, the new *N*-hexadecyl derivative **2c** performed better than the known heptyl compound **1** in three out of four tested cancer cell lines (518A2, HCT-116, Panc-1). In the vinblastine-resistant KB-V1(Vbl) cervix carcinoma cells overexpressing the Pgp transporter responsible for drug efflux as well as in the gemcitabine-resistant Panc-1 pancreas cancer cells the *N*-dodecyl derivative **2a** performed best. Compounds **1** and **2a–c** are strikingly more active in the multidrug-resistant KB-V1(Vbl) cancer cells with IC_{50} values in the nanomolar range when compared with the other three cancer cell lines. The vanillyl derivative **3c** showed distinctly lower activity when compared with **2a–c** in these four cancer cell lines.

The tumor selectivity index (SI) of **2c** is of importance for the potential clinical applicability of the compound. The SI features the ratio of the IC_{50} value against non-malignant MCF-10A breast epithelial cells ($IC_{50} > 50 \mu\text{M}$) and the tested cancer cell lines (Table 2). The greater the SI, the more selective is compound **2c**.

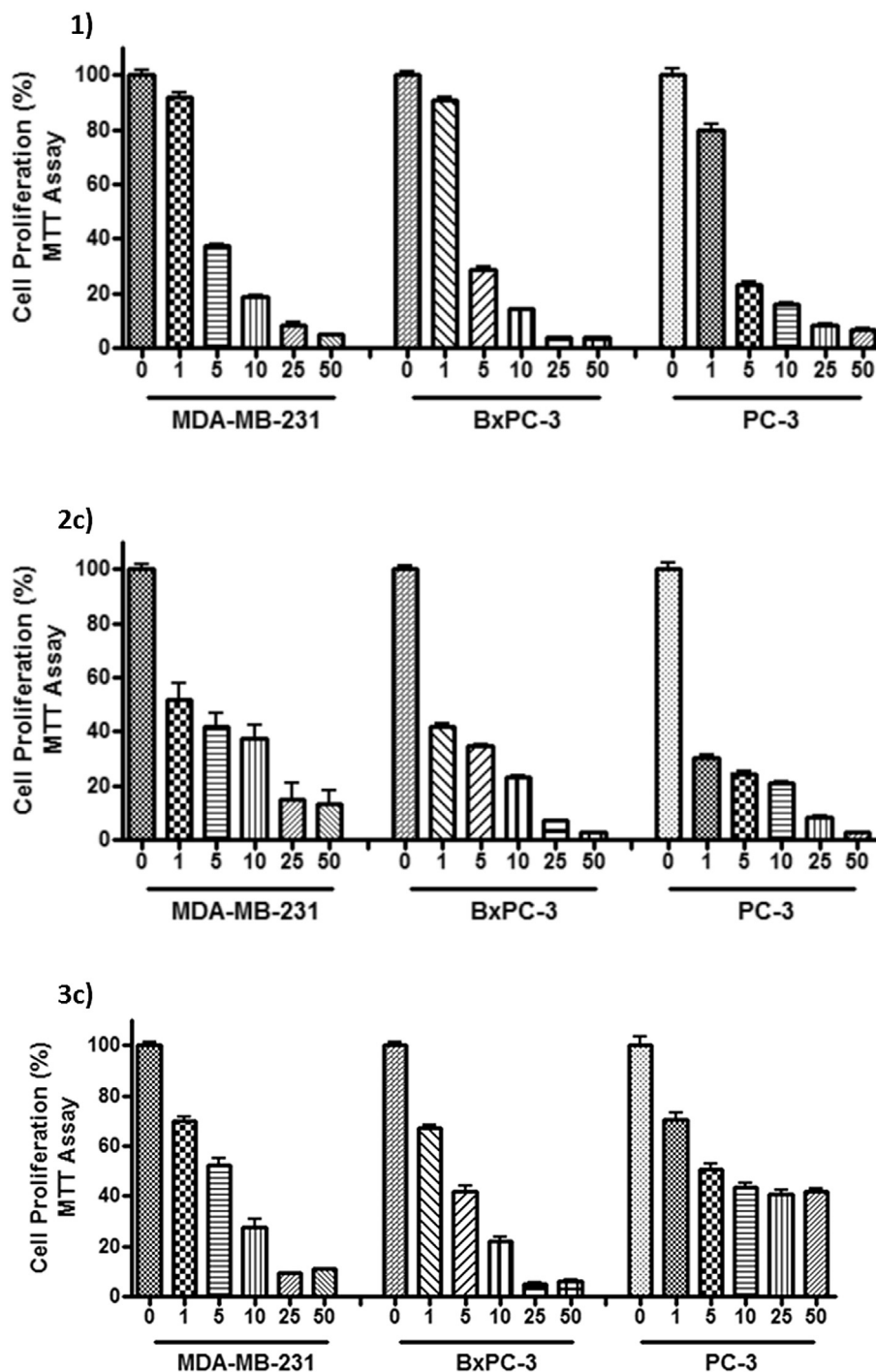


Fig. 2. Growth inhibition of compounds **1**, **2c** and **3c** after 96 h when applied to cells of human MDA-MB-231 breast carcinoma, BxPC-3 pancreas carcinoma, and PC-3 prostate carcinoma (MTT assay). X-axis: concentrations in μM.

Excellent SI values of more than 20 were calculated for **2c** in the tested cancer cell lines, and the PC-3 prostate carcinoma cells exhibited the best SI value (more than 75) for **2c**.

Since the mechanism of action of naphthoquinones is associated with the generation of reactive oxygen species (ROS), we also determined the ROS levels in 518A2 melanoma cells after treatment with compounds **1** and **2a–c** for 24 h by using the NBT assay (Fig. 4) [28–31]. 518A2 cells were incubated with 0.1 μM and 0.5 μM of the

test compounds (i.e., non-toxic concentrations after 24 h). The ROS level in cells exposed to 0.1 μM of the test compounds was on average increased by 50% when compared with untreated control cells. The ROS production in cells treated with 0.5 μM of the test compounds **1** and **2a–b** was on average even increased by 70%, whereas the ROS level in cells treated with 0.5 μM of **2c** stayed approximately on the same level when compared with the effect at a dose of 0.1 μM.

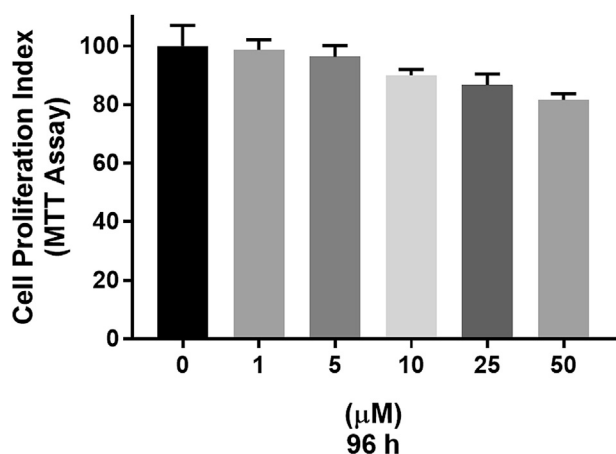


Fig. 3. Growth inhibition of compound **2c** after 96 h when applied to human MCF-10A breast epithelial cells (MTT assay).

Table 1

Inhibitory concentrations IC_{50} [μ M] of compounds **1**, **2a–e** and **3c** when applied to cells of human 518A2 melanoma, HCT-116 colon carcinoma, vinblastine-resistant KB-V1 (Vbl) cervix carcinoma, and Panc-1 pancreas carcinoma after 72 h (MTT assay).

Cell line/Compd.	518A2	HCT-116	KB-V1(Vbl)	Panc-1
1	2.58 ± 0.26	6.39 ± 0.26	0.41 ± 0.19	6.41 ± 1.10
2a	2.57 ± 0.77	3.46 ± 0.21	0.32 ± 0.04	1.79 ± 0.00
2b	3.03 ± 0.22	2.41 ± 0.21	0.43 ± 0.04	3.93 ± 0.31
2c	1.41 ± 0.33	2.08 ± 0.00	0.83 ± 0.05	2.19 ± 0.04
2d	3.05 ± 0.00	5.68 ± 0.00	1.56 ± 0.02	7.72 ± 0.46
2e	6.98 ± 0.26	6.77 ± 0.24	8.61 ± 0.20	17.61 ± 4.50
3c	12.25 ± 1.08	11.38 ± 1.33	16.76 ± 0.58	7.94 ± 1.33

2.3. Antitrypanosomal activity

The most promising anticancer active lawsone derivatives **1** and **2a–c** were selected and also tested for their trypanocidal activity against bloodstream-form *T. b. brucei* parasites by the Alamar Blue (AB) assay (Table 3). In contrast to **1**, compounds **2a–c** exhibited IC_{50} values in the sub-micromolar range. Compound **2c** was the most active compound of this series of lawsone derivatives closely followed by **2b**, and both compounds were about 10-times more active than **1**. Thus, the compound with the longest alkyl chain (**2c**) performed best against *T. b. brucei* cells just like in most tested cancer cell lines. The approved anti-leishmanial drug miltefosine also harbors a hexadecyl residue and it is possible that compound **2c** and miltefosine have certain modes of action in common (e.g., modulation of ether-lipid biosynthesis, inhibition of protein kinases and cytochrome-C-oxidase, induction of programmed cell death, cytoskeleton disruption) [32,33].

Table 2

Tumor selectivity index (SI), IC_{50} (MCF-10A, >50 μ M)/ IC_{50} (cancer cells) of compound **2c**.

Cell line	SI
518A2	>35
HCT-116	>24
KB-V1 (Vbl)	>60
Panc-1	>22
MDA-MB-231	>46
BxPC-3	>61
PC-3	>75

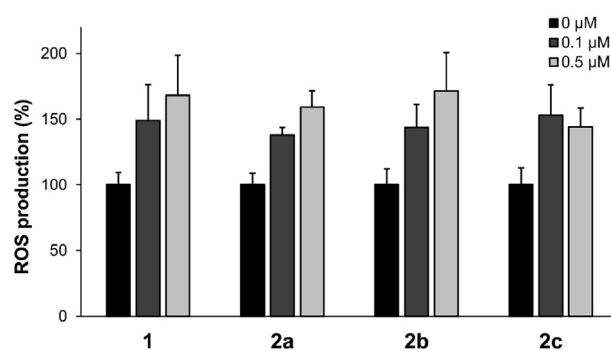


Fig. 4. Effects of compounds **1** and **2a–c** on the relative ROS level in 518A2 melanoma cells after incubation for 24 h as to NBT assays. The relative ROS production was obtained as the mean \pm SD of six independent experiments with respect to vehicle (DMSO) treated control cells (100% ROS production).

Table 3

Inhibitory concentrations IC_{50} (72 h) [μ M] of compounds **1**, **2a–c**, and pentamidine (positive control) from AB assays against cells of *T. b. brucei*. Mean of three values, standard deviation $< \pm 15\%$.

Compd.	IC_{50} [μ M]
1	3.73
2a	0.646
2b	0.350
2c	0.303
Pentamidine	0.005

The effects of the lawsone derivatives **1** and **2a–c** on the *T. b. brucei* cytoskeleton were analysed via fluorescence microscopy and the observed results harmonized well with the data obtained from the AB assays. At concentrations of 1 μ M and 10 μ M, derivative **2c** caused a deformation of the *T. b. brucei* microtubule cytoskeleton. While after 1 h many vital *T. b. brucei* cells were visible, after 3–6 h flagellae were separated from the cells and *T. b. brucei* cells were strongly deformed and rounded when compared with untreated *T. b. brucei* cells (Fig. 5, Fig. S7, Supporting information). Similar effects were observed for *T. b. brucei* cells treated with **2a** and **2b** (Figs. S8 and S9, Supporting information). In addition, reduced motility was observed from treated *T. b. brucei* cells when compared with untreated cells. Interestingly, compounds **2a–c** did not affect the cytoskeleton of human HeLa cells at high doses of 10 μ M and the treated human HeLa cells remained viable at this dose (Figs. S10–S12, Supporting information). Thus, compounds **2a–c** changed the cytoskeletal morphology of *T. b. brucei* cells in a selective way. In contrast to the active compounds **2a–c**, derivative **1** caused no significant changes of the *T. b. brucei* cell morphology at high doses (10 μ M, Fig. S13, Supporting information) which is in line with its weaker IC_{50} value when compared with **2a–c**. Prolonged incubation (12–24 h) of *T. b. brucei* cells with high dose **2b** (10 μ M) only revealed cell debris of the dead and lysed *T. b. brucei* cells (Fig. S14, Supporting information).

2.4. Antiamoebic activity

The antiamoebic activity of **2c** was investigated over three days against *Entamoeba histolytica* samples isolated from patients of the Ibrahim Malik Hospital of Khartoum, Sudan (Table 4). Compound **2c** exhibited strong time- and dose-dependent antiamoebic activity when compared with untreated cells (control). In addition, **2c** was distinctly more active (up to more than 20% higher growth

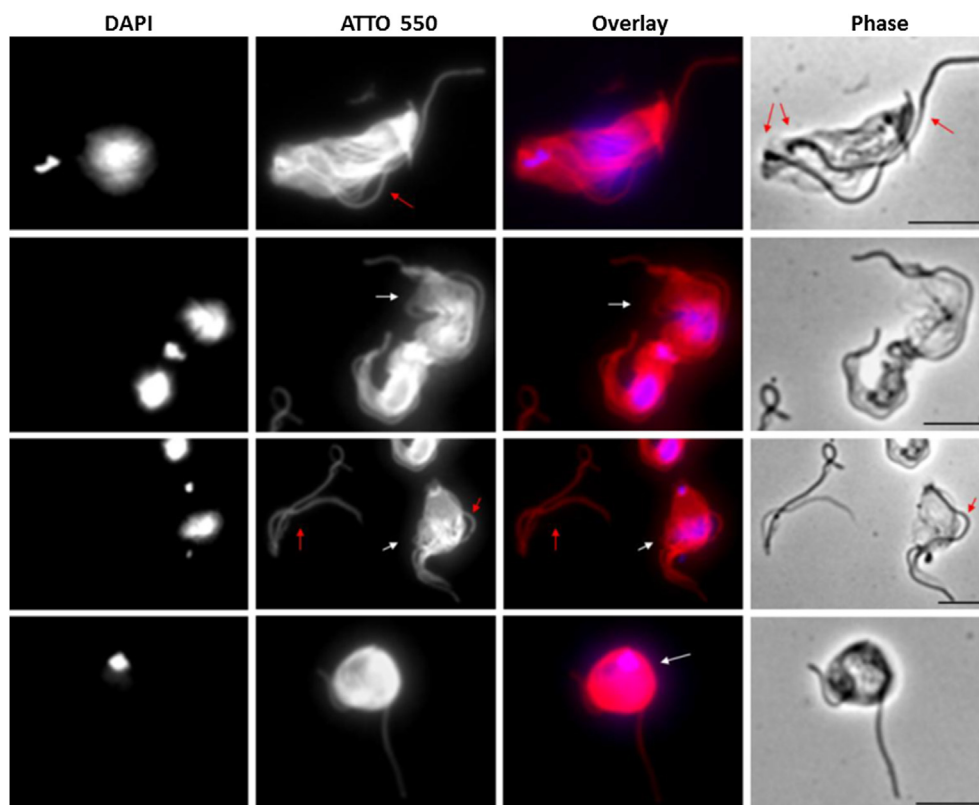


Fig. 5. Immunofluorescence images of MeOH-fixed *T. b. brucei* cells after incubation with **2c** (1 μ M) for 1 h (top row), 3 h (both central rows), and 6 h (bottom row) (bars = 10 μ m). Signals of DAPI (DNA), ATTO 550 (tubulin), the overlay of both (DAPI = blue, ATTO 550 = red) and the phase contrast (phase) are shown. White arrows indicate tubulin anomalies, red arrows mark flagellae. (For interpretation of the references to colour in this figure legend, the reader is referred to the web version of this article.)

Table 4

Growth inhibition (in %) of locally isolated strains of *Entamoeba histolytica* treated with **2c** over three days and comparison with untreated samples (control). Metronidazole (200 μ g/mL) was applied as positive control. Mean of three values, ($P < 0.05$).

Compd.	24 h	48 h	72 h
2c (100 μ g/mL)	77.8	80.9	82.8
2c (50 μ g/mL)	66.6	82.1	85.3
2c (25 μ g/mL)	60.0	66.0	70.6
Metronidazole	54.1	58.7	60.4
Control	0	5.1	11.9

inhibition) than the approved anti-parasitic drug metronidazole against the applied *Entamoeba histolytica* samples. Even the lowest dose of **2c** (25 μ g/mL) showed stronger antiamebic activity (6–10% higher growth inhibition) than metronidazole (200 μ g/mL).

3. Conclusions

Lawson was successfully employed for the synthesis of new Mannich bases that are active against a variety of cancer cell lines and parasites. The *N*-alkyl chain length is decisive for the anti-proliferative activity. While *N*-dodecyl and *N*-tetradecyl derivatives **2a** and **2b** already performed better than *N*-heptyl compound **1**, the *N*-hexadecyl compound **2c** was most active. Exceptions are the vinblastine-resistant cervix carcinoma KB-V1(Vbl) and the Panc-1 pancreas cancer cells where the *N*-dodecyl derivative **2a** was more active than the *N*-hexadecyl **2c** and the *N*-heptyl derivative **1**. Compounds **2a–c** increased the formation of ROS in cancer cells significantly. The benzyl- and 2-pyridylmethyl-amino derivatives

were generally less active. A similar activity profile was observed for the vanillyl compounds **3a–e**. The reason for the particularly high activity of compounds **2a–c** in the androgen receptor-negative PC-3 prostate cancer cells remains to be elucidated. Compound **2c** also exhibited distinct antiparasitic activity, associated with a marked deformation of the microtubule cytoskeleton of treated *T. b. brucei* parasites. This was a selective effect since human HeLa cells did not show any anomalies upon treatment with **2c**. In addition, the distinctly higher activity of **2c** in *E. histolytica* cells when compared with the antiparasitic drug metronidazole justifies further investigations of **2c** and related analogs in this field of tropical diseases. Given their simple preparation the new lawson Mannich bases **2a–c** appear to be promising multi-targeted drug candidates for the treatment of tumor and parasitic diseases.

4. Experimental

4.1. Chemistry

All starting compounds were purchased from Aldrich. Compounds **1** and **2e** were prepared according to a literature procedure [19,27]. The following instruments were used: melting points (uncorrected), Gallenkamp; IR spectra, Perkin-Elmer Spectrum One FT-IR spectrophotometer with ATR sampling unit; nuclear magnetic resonance spectra, BRUKER Avance 300 spectrometer; chemical shifts are given in parts per million (δ) downfield from tetramethylsilane as internal standard; mass spectra, Varian MAT 311A (EI), UPLC/Orbitrap (ESI); microanalyses, Perkin-Elmer 2400 CHN elemental analyzer. All tested compounds are >95% pure by elemental analysis.

4.1.1. 3-[(Dodecylamino)(2-pyridyl)methyl]-2-hydroxy-1,4-naphthoquinone (**2a**)

2-Hydroxy-1,4-naphthoquinone (435 mg, 2.5 mmol) was suspended in EtOH (15 mL), dodecylamine (510 mg, 2.75 mmol) was added and the resulting solution was stirred at room temperature for 5 min. Pyridine-2-carboxaldehyde (287 μ L, 3.0 mmol) was added and the reaction mixture was stirred at room temperature for 5 h. The formed precipitate was collected, washed with EtOH and dried in vacuum. Yield: 800 mg (1.78 mmol, 71%); orange-red solid of mp 140–141 °C; ν_{\max} (ATR)/ cm^{-1} 3117, 2956, 2921, 2851, 1682, 1582, 1530, 1506, 1471, 1434, 1409, 1387, 1272, 1230, 1155, 1145, 1092, 1064, 1044, 990, 920, 889, 867, 844, 822, 793, 770, 748, 733, 697, 665; ^1H NMR (300 MHz, CDCl_3) δ 0.85 (3H, t, $J = 6.5$ Hz), 1.2–1.4 (18H, m), 1.8–1.9 (2H, m), 3.0–3.1 (1H, m), 3.2–3.3 (1H, m), 5.70 (1H, s), 7.1–7.2 (1H, m), 7.3–7.4 (2H, m), 7.44 (1H, dd, $J = 7.5$ Hz), 7.57 (1H, dd, $J = 7.7$ Hz), 7.7–7.8 (2H, m), 8.4–8.5 (1H, m), 9.4–9.6 (1H, br s); ^{13}C NMR (75.5 MHz, CDCl_3) δ 14.1, 22.7, 26.6, 26.9, 29.1, 29.3, 29.4, 29.5, 29.6, 31.9, 47.1, 59.1, 111.0, 122.4, 122.9, 125.4, 126.2, 131.0, 131.4, 133.6, 134.2, 137.6, 147.6, 155.4, 170.9, 181.1, 184.7; m/z (%) 274 (12), 218 (37), 174 (27), 119 (100), 92 (32).

4.1.2. 3-[(Tetradecylamino)(2-pyridyl)methyl]-2-hydroxy-1,4-naphthoquinone (**2b**)

Analogously to the synthesis of **2a**, compound **2b** was obtained from 2-hydroxy-1,4-naphthoquinone (435 mg, 2.5 mmol), tetradecylamine (587 mg, 2.75 mmol) and pyridine-2-carboxaldehyde (287 μ L, 3.0 mmol) in EtOH (15 mL). Yield: 790 mg (1.66 mmol, 66%); red solid of mp 116–118 °C; ν_{\max} (ATR)/ cm^{-1} 3120, 2920, 2851, 1682, 1589, 1581, 1528, 1503, 1469, 1434, 1409, 1384, 1272, 1232, 1157, 1145, 1092, 1060, 1044, 991, 965, 907, 894, 844, 821, 793, 769, 747, 733, 697, 664; ^1H NMR (300 MHz, CDCl_3) δ 0.85 (3H, t, $J = 6.6$ Hz), 1.2–1.4 (22H, m), 1.8–2.0 (2H, m), 3.0–3.1 (1H, m), 3.2–3.3 (1H, m), 5.71 (1H, s), 7.0–7.1 (1H, m), 7.3–7.4 (3H, m), 7.54 (1H, dd, $J = 7.9$ Hz), 7.7–7.8 (2H, m), 8.4–8.5 (1H, m), 9.4–9.6 (1H, br s); ^{13}C NMR (75.5 MHz, CDCl_3) δ 14.1, 22.6, 26.6, 26.8, 29.0, 29.3, 29.4, 29.5, 29.6, 31.9, 47.1, 58.9, 111.5, 122.3, 122.7, 125.3, 126.1, 130.8, 131.2, 133.5, 134.2, 137.4, 147.7, 155.5, 170.6, 180.9, 184.8; m/z (%) 302 (7), 246 (23), 119 (100).

4.1.3. 3-[(Hexadecylamino)(2-pyridyl)methyl]-2-hydroxy-1,4-naphthoquinone (**2c**)

Analogously to the synthesis of **2a**, compound **2c** was obtained from 2-hydroxy-1,4-naphthoquinone (435 mg, 2.5 mmol), hexadecylamine (664 mg, 2.75 mmol) and pyridine-2-carboxaldehyde (287 μ L, 3.0 mmol) in EtOH (15 mL). Yield: 780 mg (1.55 mmol, 62%); orange-red solid of mp 125–126 °C; ν_{\max} (ATR)/ cm^{-1} 3125, 2919, 2850, 2607, 1682, 1580, 1567, 1528, 1498, 1469, 1434, 1420, 1411, 1390, 1333, 1271, 1230, 1159, 1145, 1058, 1044, 987, 969, 912, 891, 843, 821, 792, 768, 746, 732, 697, 665; ^1H NMR (300 MHz, CDCl_3) δ 0.85 (3H, t, $J = 6.5$ Hz), 1.2–1.4 (26H, m), 1.8–2.0 (2H, m), 3.0–3.1 (1H, m), 3.2–3.3 (1H, m), 5.70 (1H, s), 7.0–7.1 (1H, m), 7.2–7.4 (3H, m), 7.5–7.6 (1H, m), 7.7–7.8 (2H, m), 8.4–8.5 (1H, m), 9.4–9.5 (1H, br s); ^{13}C NMR (75.5 MHz, CDCl_3) δ 14.1, 22.7, 26.7, 26.9, 29.1, 29.3, 29.4, 29.5, 29.6, 29.7, 31.9, 47.2, 58.9, 111.6, 122.4, 122.7, 125.3, 126.1, 130.8, 131.2, 133.5, 134.2, 137.4, 147.7, 155.5, 170.6, 180.9, 184.8; m/z (%) 330 (8), 274 (20), 119 (100).

4.1.4. 3-[(3,4-Difluorobenzylamino)(2-pyridyl)methyl]-2-hydroxy-1,4-naphthoquinone (**2d**)

Analogously to the synthesis of **2a**, compound **2d** was obtained from 2-hydroxy-1,4-naphthoquinone (435 mg, 2.5 mmol), 3,4-difluorobenzyl amine (325 μ L, 2.75 mmol) and pyridine-2-carboxaldehyde (287 μ L, 3.0 mmol) in EtOH (5 mL). Yield: 442 mg (1.09 mmol, 44%); orange-red solid of mp 148 °C; ν_{\max} (ATR)/ cm^{-1} 3032, 2959, 2326, 1682, 1611, 1589, 1560, 1518, 1470,

1454, 1434, 1385, 1374, 1351, 1315, 1288, 1274, 1262, 1210, 1206, 1164, 1151, 1141, 1118, 1099, 1077, 1045, 995, 953, 934, 906, 879, 834, 820, 813, 789, 774, 754, 735, 716, 699, 661; ^1H NMR (300 MHz, $\text{DMSO}-d_6$) δ 4.1–4.2 (2H, m), 5.65 (1H, s), 7.3–7.6 (6H, m), 7.6–7.8 (2H, m), 7.8–8.0 (2H, m), 8.5–8.6 (1H, m), 9.4–9.6 (1H, br s); ^{13}C NMR (75.5 MHz, $\text{DMSO}-d_6$) δ 47.4, 57.3, 109.4, 117.4–117.6 (m), 119.4–119.6 (m), 121.5, 122.8, 125.1–125.5 (m), 127.5, 129.9, 130.9, 131.7, 133.7, 134.7, 137.4, 147.7, 156.9, 171.2, 178.8, 184.0; m/z (%) 406 [M^+] (1), 388 (3), 265 (22), 263 (25), 237 (17), 232 (16), 216 (75), 192 (38), 180 (57), 174 (34), 142 (32), 127 (100), 105 (52), 76 (49), 52 (53).

4.1.5. 3-[(Heptylamino)(4-hydroxy-3-methoxyphenyl)methyl]-2-hydroxy-1,4-naphthoquinone (**3a**)

Analogously to the synthesis of **2a**, compound **3a** was obtained from 2-hydroxy-1,4-naphthoquinone (435 mg, 2.5 mmol), heptylamine (408 μ L, 2.75 mmol) and vanillin (456 mg, 3.0 mmol) in EtOH (15 mL). Yield: 717 mg (1.69 mmol, 68%); orange-red solid of mp 165–166 °C; ν_{\max} (ATR)/ cm^{-1} 3326, 2932, 2858, 2600, 1671, 1609, 1588, 1567, 1516, 1459, 1436, 1365, 1264, 1238, 1219, 1160, 1128, 1037, 962, 824, 804, 775, 740, 696, 660; ^1H NMR (300 MHz, $\text{CDCl}_3/\text{DMSO}-d_6$) δ 0.76 (3H, t, $J = 6.9$ Hz), 1.1–1.3 (8H, m), 1.5–1.7 (2H, m), 2.8–2.9 (3H, m), 3.73 (3H, s), 5.36 (1H, s), 6.72 (1H, d, $J = 8.2$ Hz), 6.98 (1H, dd, $J = 8.2$ Hz, 1.8 Hz), 7.11 (1H, d, $J = 1.8$ Hz), 7.3–7.4 (1H, m), 7.4–7.6 (1H, m), 7.8–7.9 (2H, m), 8.02 (1H, s), 8.9–9.0 (1H, br s), 10.6–10.7 (1H, br s); ^{13}C NMR (75.5 MHz, $\text{CDCl}_3/\text{DMSO}-d_6$) δ 13.4, 21.8, 25.8, 25.9, 28.0, 30.8, 45.8, 55.3, 60.2, 111.0, 111.8, 114.7, 120.4, 124.8, 125.3, 128.8, 130.3, 131.1, 133.0, 133.9, 146.2, 146.9, 170.0, 180.1, 184.3; m/z (%) 308 (14), 280 (36), 249 (23), 220 (47), 206 (100), 178 (61), 164 (71), 151 (38), 137 (57), 41 (48).

4.1.6. 3-[(Dodecylamino)(4-hydroxy-3-methoxyphenyl)-methyl]-2-hydroxy-1,4-naphthoquinone (**3b**)

Analogously to the synthesis of **2a**, compound **3b** was obtained from 2-hydroxy-1,4-naphthoquinone (435 mg, 2.5 mmol), dodecylamine (510 mg, 2.75 mmol) and vanillin (456 mg, 3.0 mmol), dissolved in 2 mL hot EtOH in EtOH (15 mL). Yield: 840 mg (1.70 mmol, 68%); orange-red solid of mp 165–166 °C; ν_{\max} (ATR)/ cm^{-1} 3354, 2924, 2852, 2583, 1668, 1610, 1588, 1569, 1517, 1459, 1435, 1365, 1264, 1236, 1217, 1158, 1129, 1064, 1037, 978, 883, 824, 801, 775, 738, 720, 695, 660; ^1H NMR (300 MHz, $\text{DMSO}-d_6$) δ 0.84 (3H, t, $J = 6.5$ Hz), 1.1–1.3 (18H, m), 1.5–1.6 (2H, m), 2.81 (2H, t, $J = 7.8$ Hz), 3.74 (3H, s), 5.38 (1H, s), 6.70 (1H, d, $J = 8.2$ Hz), 6.96 (1H, dd, $J = 8.2$ Hz, 2.0 Hz), 7.21 (1H, d, $J = 2.0$ Hz), 7.5–7.6 (1H, m), 7.7–7.8 (1H, m), 7.8–7.9 (2H, m), 9.0–9.1 (1H, br s); ^{13}C NMR (75.5 MHz, $\text{DMSO}-d_6$) δ 13.9, 22.1, 25.5, 25.9, 28.4, 28.7, 28.9, 29.0, 31.3, 45.4, 55.7, 58.8, 111.5, 112.6, 115.1, 120.8, 125.1125.3, 129.4, 130.8, 131.5, 133.7, 134.7, 146.5, 147.3, 170.6, 178.5, 184.4; m/z (%) 319 (22), 308 (18), 280 (43), 234 (17), 220 (52), 206 (100), 178 (53), 164 (63), 151 (32), 137 (53), 105 (34), 76 (15), 55 (21), 44 (23).

4.1.7. 3-[(Hexadecylamino)(4-hydroxy-3-methoxyphenyl)-methyl]-2-hydroxy-1,4-naphthoquinone (**3c**)

Analogously to the synthesis of **2a**, compound **3c** was obtained from 2-hydroxy-1,4-naphthoquinone (435 mg, 2.5 mmol), hexadecylamine (664 mg, 2.75 mmol) and vanillin (456 mg, 3.0 mmol), dissolved in 2 mL hot EtOH in EtOH (15 mL). Yield: 910 mg (1.66 mmol, 66%); orange-red solid of mp 159–160 °C; ν_{\max} (ATR)/ cm^{-1} 3375, 2918, 2850, 1671, 1612, 1589, 1575, 1517, 1450, 1365, 1267, 1237, 1215, 1162, 1126, 1038, 988, 924, 887, 869, 844, 832, 806, 794, 777, 738, 719, 694, 661; ^1H NMR (300 MHz, $\text{DMSO}-d_6$) δ 0.84 (3H, t, $J = 6.5$ Hz), 1.1–1.3 (26H, m), 1.5–1.6 (2H, m), 2.81 (2H, t, $J = 7.6$ Hz), 3.73 (3H, s), 5.38 (1H, s), 6.70 (1H, d, $J = 8.2$ Hz), 6.96 (1H, dd, $J = 8.2$ Hz, 2.0 Hz), 7.21 (1H, d, $J = 2.0$ Hz), 7.5–7.6 (1H, m), 7.6–7.7 (1H, m), 7.8–7.9 (2H, m), 9.0–9.1 (1H, br s); ^{13}C NMR (75.5 MHz, $\text{DMSO}-d_6$) δ 13.9, 22.1, 25.4, 25.8, 28.4, 28.7, 28.9, 29.0,

31.3, 45.4, 55.7, 58.9, 111.5, 112.6, 115.1, 120.8, 125.1125.3, 129.3, 130.8, 131.5, 133.7, 134.7, 146.6, 147.3, 170.6, 178.5, 184.4; m/z (%) 550.35 (100) [M^+], 242.28 (87).

4.1.8. 3-[(Benzylamino)(4-hydroxy-3-methoxyphenyl)-methyl]-2-hydroxy-1,4-naphthoquinone (**3d**)

Analogously to the synthesis of **2a**, compound **3d** was obtained from 2-hydroxy-1,4-naphthoquinone (435 mg, 2.5 mmol), benzylamine (300 μ L, 2.75 mmol) and vanillin (456 mg, 3.0 mmol, dissolved in 2 mL hot EtOH) in EtOH (15 mL). Yield: 450 mg (1.08 mmol, 43%); orange-red solid of mp 180–181 °C; ν_{\max} (ATR)/ cm^{-1} 3117, 3070, 3030, 2965, 2590, 1675, 1618, 1590, 1552, 1519, 1478, 1456, 1429, 1370, 1329, 1279, 1254, 1225, 1154, 1125, 1089, 1064, 1031, 979, 948, 934, 918, 869, 818, 795, 759, 736, 703, 662; ^1H NMR (300 MHz, DMSO- d_6) δ 3.72 (3H, s), 4.0–4.1 (2H, m), 5.39 (1H, s), 6.71 (1H, d, J = 8.2 Hz), 6.91 (1H, dd, J = 8.2 Hz, 2.0 Hz), 7.14 (1H, d, J = 2.0 Hz), 7.3–7.4 (5H, m), 7.5–7.8 (2H, m), 7.8–8.0 (2H, m), 9.0–9.1 (1H, br s); ^{13}C NMR (75.5 MHz, DMSO- d_6) δ 48.9, 55.7, 58.8, 111.3, 112.6, 115.2, 120.9, 125.0, 125.3, 128.5, 128.7, 129.0, 129.9, 130.8, 131.6, 132.4, 133.6, 134.6, 146.7, 147.3, 170.5, 178.6, 184.2; m/z (%) 416.15 [M^+] (100), 309.08 (90).

4.1.9. 3-[(2-Pyridylmethylamino)(4-hydroxy-3-methoxy-phenyl)-methyl]-2-hydroxy-1,4-naphthoquinone (**3e**)

Analogously to the synthesis of **2a**, compound **3e** was obtained from 2-hydroxy-1,4-naphthoquinone (435 mg, 2.5 mmol), 2-pyridylmethylamine (280 μ L, 2.75 mmol) and vanillin (456 mg, 3.0 mmol, dissolved in 2 mL hot EtOH) in EtOH (15 mL). Yield: 400 mg (0.98 mmol, 39%); orange-red solid of mp 153–155 °C; ν_{\max} (ATR)/ cm^{-1} 3131, 3071, 2956, 1677, 1614, 1591, 1553, 1520, 1477, 1429, 1387, 1369, 1280, 1249, 1229, 1162, 1132, 1038, 996, 953, 871, 836, 799, 774, 757, 739, 696, 660; ^1H NMR (300 MHz, DMSO- d_6) δ 3.72 (3H, s), 4.2–4.3 (2H, m), 5.54 (1H, s), 6.72 (1H, d, J = 8.2 Hz), 6.97 (1H, dd, J = 8.2 Hz, 2.0 Hz), 7.21 (1H, d, J = 2.0 Hz), 7.3–7.4 (2H, m), 7.5–7.6 (1H, m), 7.6–7.7 (1H, m), 7.8–7.9 (3H, m), 8.6–8.7 (1H, m), 9.0–9.1 (1H, br s), 9.9–10.1 (1H, br s); ^{13}C NMR (75.5 MHz, DMSO- d_6) δ 48.8, 55.6, 59.1, 111.4, 112.8, 115.2, 121.0, 122.1, 122.2, 123.3, 125.1125.3, 128.7, 130.8, 131.6, 133.7, 134.6, 137.3, 146.7, 147.3, 148.9, 152.6, 170.7, 178.6, 184.3; m/z (%) 417.14 [M^+] (55), 309.08 (100).

4.1.10. 3-[(Heptylamino)(3,4-difluorophenyl)methyl]-2-hydroxy-1,4-naphthoquinone (**4a**)

Analogously to the synthesis of **2a**, compound **4a** was obtained from 2-hydroxy-1,4-naphthoquinone (435 mg, 2.5 mmol), heptylamine (408 μ L, 2.75 mmol) and 3,4-difluorobenzaldehyde (330 μ L, 3.0 mmol) in EtOH (15 mL). Yield: 960 mg (2.32 mmol, 93%); orange solid of mp 155–157 °C; ν_{\max} (ATR)/ cm^{-1} 2960, 2935, 2865, 2841, 2362, 1673, 1612, 1591, 1568, 1528, 1514, 1464, 1451, 1434, 1366, 1331, 1270, 1243, 1226, 1116, 1083, 1070, 1014, 973, 944, 913, 890, 876, 862, 841, 823, 801, 786, 756, 731, 711, 690, 660; ^1H NMR (300 MHz, DMSO- d_6) δ 0.80 (3H, t, J = 6.9 Hz), 1.0–1.1 (8H, m), 1.5–1.7 (2H, m), 2.84 (2H, t, J = 7.6 Hz), 5.50 (1H, s), 7.4–7.5 (2H, m), 7.5–7.6 (1H, m), 7.6–7.7 (2H, m), 7.8–7.9 (1H, m), 7.9–8.0 (1H, m); ^{13}C NMR (75.5 MHz, DMSO- d_6) δ 13.9, 21.9, 25.5, 25.8, 28.1, 30.9, 45.7, 57.7, 110.6, 116.7–117.4 (m), 124.9–125.4 (m), 130.9, 131.5, 133.8, 134.6, 135.9, 136.3, 147.4, 170.7, 178.3, 184.2; m/z (%) 413 (1) [M^+], 378 (2), 298 (11), 271 (100), 270 (96), 242 (28), 214 (45), 196 (38), 104 (40), 76 (35).

4.1.11. 3-[(Dodecylamino)(3,4-difluorophenyl)methyl]-2-hydroxy-1,4-naphthoquinone (**4b**)

Analogously to the synthesis of **2a**, compound **4b** was obtained from 2-hydroxy-1,4-naphthoquinone (435 mg, 2.5 mmol), dodecylamine (510 mg, 2.75 mmol) and 3,4-difluorobenzaldehyde

(330 μ L, 3.0 mmol) in EtOH (15 mL). Yield: 990 mg (2.05 mmol, 82%); orange-red solid of mp 157–158 °C; ν_{\max} (ATR)/ cm^{-1} 3126, 2927, 2856, 2686, 1681, 1605, 1576, 1510, 1475, 1427, 1397, 1381, 1347, 1274, 1227, 1158, 1141, 1120, 1094, 1048, 995, 957, 873, 832, 823, 800, 785, 762, 737, 722, 697, 657; ^1H NMR (300 MHz, CDCl_3) δ 0.82 (3H, t, J = 6.6 Hz), 1.1–1.3 (18H, m), 1.6–1.8 (2H, m), 2.8–3.0 (1H, m), 3.1–3.2 (1H, m), 5.6–5.8 (1H, br s), 6.8–6.9 (1H, m), 7.1–7.2 (1H, m), 7.4–7.6 (3H, m), 7.9–8.0 (2H, m), 9.6–9.8 (1H, br s); ^{13}C NMR (75.5 MHz, CDCl_3) δ 14.1, 22.6, 26.6, 26.9, 29.0, 29.3, 29.4, 29.5, 29.6, 31.9, 46.8, 59.4, 112.1, 116.7–117.2 (m), 124.1, 125.8–126.2 (m), 131.2–131.5 (m), 134.0, 134.3, 134.9, 148.3, 151.6, 169.4, 181.7, 185.5; m/z (%) 308 (3), 270 (17), 210 (22), 196 (100), 168 (33), 154 (54), 127 (55), 104 (8), 76 (9), 55 (17), 41 (22).

4.1.12. 3-[(Tetradecylamino)(3,4-difluorophenyl)methyl]-2-hydroxy-1,4-naphthoquinone (**4c**)

Analogously to the synthesis of **2a**, compound **4c** was obtained from 2-hydroxy-1,4-naphthoquinone (435 mg, 2.5 mmol), tetradecylamine (587 mg, 2.75 mmol) and 3,4-difluorobenzaldehyde (330 μ L, 3.0 mmol) in EtOH (15 mL). Yield: 600 mg (1.17 mmol, 47%); orange solid of mp 121–122 °C; ν_{\max} (ATR)/ cm^{-1} 2925, 2853, 2571, 2400, 1666, 1612, 1590, 1534, 1517, 1486, 1470, 1435, 1366, 1326, 1314, 1273, 1262, 1249, 1230, 1119, 971, 876, 868, 836, 825, 803, 758, 732, 710, 691, 660; ^1H NMR (300 MHz, CDCl_3) δ 0.83 (3H, t, J = 6.6 Hz), 1.0–1.3 (22H, m), 1.6–1.8 (2H, m), 2.9–3.0 (1H, m), 3.1–3.2 (1H, m), 5.6–5.8 (1H, br s), 6.8–6.9 (1H, m), 7.1–7.2 (1H, m), 7.4–7.6 (3H, m), 7.9–8.1 (2H, m), 9.6–9.8 (1H, br s); ^{13}C NMR (75.5 MHz, CDCl_3) δ 14.1, 22.6, 26.5, 26.9, 29.0, 29.3, 29.4, 29.5, 29.6, 31.9, 46.9, 59.3, 111.9, 116.9–117.1 (m), 124.0, 125.8–126.2 (m), 131.2–131.6 (m), 134.0, 134.3, 135.1, 145.1, 148.3, 151.5, 169.3, 181.9, 185.5; m/z (%) 512.30 [M^+] (100).

4.1.13. 3-[(Hexadecylamino)(3,4-difluorophenyl)methyl]-2-hydroxy-1,4-naphthoquinone (**4d**)

Analogously to the synthesis of **2a**, compound **4d** was obtained from 2-hydroxy-1,4-naphthoquinone (435 mg, 2.5 mmol), hexadecylamine (664 mg, 2.75 mmol) and 3,4-difluorobenzaldehyde (330 μ L, 3.0 mmol) in EtOH (15 mL). Yield: 970 mg (1.80 mmol, 72%); orange solid of mp 127–128 °C; ν_{\max} (ATR)/ cm^{-1} 2923, 2853, 2420, 1667, 1613, 1589, 1534, 1517, 1468, 1437, 1364, 1311, 1258, 1227, 119, 972, 875, 823, 803, 772, 758, 732, 710, 691, 660; ^1H NMR (300 MHz, CDCl_3) δ 0.84 (3H, t, J = 6.5 Hz), 1.1–1.3 (26H, m), 1.6–1.8 (2H, m), 2.9–3.0 (1H, m), 3.1–3.2 (1H, m), 5.6–5.8 (1H, br s), 6.8–6.9 (1H, m), 7.1–7.2 (1H, m), 7.4–7.6 (3H, m), 7.9–8.1 (2H, m), 9.6–9.8 (1H, br s); ^{13}C NMR (75.5 MHz, CDCl_3) δ 14.1, 22.7, 26.6, 26.9, 29.0, 29.3, 29.5, 29.6, 31.9, 46.9, 59.3, 111.9, 116.9–117.1 (m), 124.0, 125.8–126.2 (m), 131.2–131.6 (m), 134.0, 134.3, 135.2, 145.1, 148.3, 151.5, 169.3, 181.9, 185.5; m/z (%) 540.33 (100) [M^+].

4.1.14. 3-[(2-Pyridylmethylamino)(3,4-difluorophenyl)methyl]-2-hydroxy-1,4-naphthoquinone (**4e**)

Analogously to the synthesis of **2a**, compound **4e** was obtained from 2-hydroxy-1,4-naphthoquinone (435 mg, 2.5 mmol), 2-pyridylmethylamine (280 μ L, 2.75 mmol) and 3,4-difluorobenzaldehyde (330 μ L, 3.0 mmol) in EtOH (15 mL). Yield: 500 mg (1.23 mmol, 49%); orange solid of mp 141–142 °C; ν_{\max} (ATR)/ cm^{-1} 3055, 3003, 2976, 2324, 1679, 1591, 1565, 1513, 1474, 1437, 1369, 1320, 1271, 1246, 1226, 1162, 1147, 1116, 1075, 1053, 1025, 997, 962, 938, 873, 845, 822, 800, 769, 756, 733, 710, 690, 660; ^1H NMR (300 MHz, DMSO- d_6) δ 4.2–4.4 (2H, m), 5.67 (1H, s), 7.3–7.5 (4H, m), 7.6–7.8 (3H, m), 7.8–8.0 (3H, m), 8.6–8.7 (1H, m), 10.0–10.2 (1H, br s); ^{13}C NMR (75.5 MHz, DMSO- d_6) δ 49.41, 58.0, 110.6, 117.0–117.6 (m), 122.3–122.5 (m), 123.1, 123.4, 125.1, 125.4, 125.7, 131.0, 131.6, 131.9, 133.7, 134.5, 137.2, 149.0, 152.3, 170.7, 178.5, 184.1; m/z (%) 388 (34), 386 (16), 321 (21), 300 (100), 286 (21), 181

(27), 174 (34), 105 (37), 93 (35), 77 (30).

4.2. Cell lines and culture conditions

PC-3 prostate cancer cells, BxPC-3 pancreatic cancer cells and MDA-MB-231 breast cancer cells were purchased from the American Type Culture Collection (Manassas, VA) and maintained in Dulbecco's modified Eagle's medium (DMEM; Invitrogen, Carlsbad, CA) supplemented with 10% fetal calf serum (FCS), 100 units/mL of penicillin, and 100 µg/mL of streptomycin in a 5% CO₂ atmosphere at 37 °C. The human MCF-10A breast epithelial cells (obtained from ATCC) were maintained in DMEM-F12 medium supplemented with 0.1 µg/mL cholera toxin, 0.02 µg/mL epidermal growth factor, 10 µg/mL insulin, 0.5 µg/mL hydrocortisone, 100 U/mL penicillin, 100 µg/mL streptomycin and 5% horse serum in a humidified 5% CO₂ atmosphere at 37 °C. The human melanoma cell line 518A2 was obtained from the Department of Radiotherapy, Medical University of Vienna, Austria. The KB-V1(Vbl) cells were obtained from the Institute of Pharmacy of the University Regensburg, Germany, and the colon HT-29 cells and HCT-116 cells from the University Hospital Erlangen, Germany. The HCT-116 colon cancer cells were grown in Roswell Park Memorial Institute medium 1640 (RPMI-1640) supplemented with 10% FCS, 100 IU/mL penicillin G, 100 µg/mL streptomycin sulfate, 0.25 µg/mL amphotericin B, and 250 µg/mL gentamycin (all from Gibco, Eggenstein, Germany). The 518A2 and the KB-V1/Vbl cells were cultured in DMEM containing 10% FCS, 100 IU/mL penicillin G, 100 µg/mL streptomycin sulfate, 0.25 µg/mL amphotericin B, and 250 µg/mL gentamycin. The cells were maintained in a moisture saturated atmosphere (5% CO₂) at 37 °C. They were serially passaged following trypsinization with 0.05% trypsin/0.02% EDTA (PAA Laboratories, Coelbe, Germany). Mycoplasma contamination was routinely monitored, and only mycoplasma-free cultures were used.

4.3. MTT assay

3-(4,5-Dimethylthiazol-2-yl)-2,5-diphenyltetrazolium bromide (MTT; ABCR) was used to identify viable cells that reduce it to a violet formazan [34]. The adherent 518A2 melanoma, HCT-116, and KB-V1(Vbl) cells (5×10^4 cells/mL), the MCF-10A cells (4×10^3 cells/well) and PC-3 cells (3×10^3 cells/well), BxPC-3 cells (3×10^3 cells/well) and MDA-MB-231 cells (3×10^3 cells/well) were seeded and cultured for 24 h on 96-well microplates. Incubation (5% CO₂, 95% humidity, 37 °C) of cells following treatment with the test compounds (dilution series ranging from 0.0001 to 100 µM in DMSO) was continued for 72 h or 96 h. Solvent controls were incubated under identical conditions. In the case of PC-3, BxPC-3, MDA-MB-231 and MCF-10A cells, 25 µL of MTT stock solution, containing 5 mg/mL in phosphate-buffered saline (PBS), was added to a final concentration of 0.05% and incubated for further 2 h at 37 °C. The supernatant was aspirated, and the formazan was dissolved in isopropanol or DMSO (100 µL). The absorbance at 595 nm was measured on an Ultra Multifunctional Microplate Reader (TECAN, Durham, NC). In the case of KB-V1(Vbl) cells, a 5 mg/mL stock solution of MTT in PBS was added to a final MTT concentration of 0.05% (518A2) or 0.1%. After 2 h, the microplates were swiftly turned, flicked, and blotted to discard the medium whereupon the precipitate of formazan crystals was redissolved in a 10% solution of sodium dodecylsulfate in DMSO containing 0.6% acetic acid. The microplates were gently shaken in the dark for 30 min and left in the incubator overnight to ensure a complete dissolution of the formazan. The absorbance at 570 and 630 nm was measured using an automatic ELISA microplate reader (MWG-BIOTECH). All experiments were carried out at least in triplicate, and the percentage of viable cells quoted was calculated as the mean SD with respect to

the controls set to 100%.

4.4. NBT assay

The NBT assay was used to determine the ROS levels in 518A2 melanoma cells after treatment with vehicle (DMSO) or the test compounds (**1**, **2a–c**) as previously described [35]. 518A2 melanoma cells (1×10^5 cells/mL; 100 µL/well) were grown in 96-well plates for 24 h at 37 °C. Then, the cells were exposed to test compounds **1** and **2a–c** (0, 0.1, and 0.5 µM) for another 24 h. After centrifugation (300 g; 5 min), the medium was aspirated and the cells were incubated for 4 h at 37 °C with 25 µL of a 0.1% NBT solution in PBS. Then, the supernatant was withdrawn and the cells lysed in 25 µL of a 2 M KOH solution and the formazan dissolved in 33 µL DMSO. The absorbance at 630 nm (formazan) and at 405 nm (background) were measured with a microplate reader (Tecan) after 30 min of incubation at 37 °C. All experiments were done in sextuplicate. The relative ROS production was calculated as the mean ± SD relative to vehicle treated control cells, which were set to 100%.

4.5. Trypanosoma and human HeLa cell lines and culture conditions

Cells of the *T. b. brucei* bloodstream trypomastigote cell line 65.3 were maintained in HMI-9 medium, pH 7.5, supplemented with heat-inactivated 10% fetal bovine serum (FBS) and 5% Serum Plus (Sigma-Aldrich) in a humidified 5% CO₂ atmosphere at 37 °C. The human HeLa cells were grown in DMEM medium, supplemented with 4.5 g/L glucose + 2 mM L-glutamine, 0.5% FBS, 0.05% streptomycin and penicillin in a humidified 5% CO₂ atmosphere at 37 °C.

4.6. Alamar Blue (AB) assay

The AB assay was used to identify viable cells after treatment with drug candidates [36–39]. This assay bases on the irreversible reaction of the blue dye resazurin and NADH to pink resofurin in intact cells. *T. b. brucei* cells (4×10^5 /well) were seeded on 96-well microplates, treated with the test compounds (dissolved in DMSO) and incubated for 72 h (5% CO₂, 95% humidity, 37 °C). 10 µL of the AB reagent (500 µM resazurin sodium salt in PBS) was added and incubated for further 4–8 h at 37 °C. The fluorescence (extinction at 544 nm, emission at 590 nm) was measured on an Omega Fluostar (BMG Labtech) fluorescence plate reader.

4.7. Immunofluorescence staining of HeLa cells and trypanosomes

The DMEM medium was removed from HeLa cell cultures and the cells were washed with phosphate-buffered saline (PBS). Trypsin-EDTA (1 mL) was added and the cells were incubated for 2 min at 37 °C. The cells were taken up in DMEM medium (9 mL) and centrifuged for 2 min at 1250×g. The supernatant was discarded and the cell pellet suspended in DMEM medium (9 mL). 0.5 mL of the cell suspension was added to each well (containing 1.5 mL DMEM) of a 12-well plate at 37 °C (total volume in each well = 2 mL), then a round glass coverslip (diameter of 18 mm) pretreated with 70% ethanol was laid into the wells, and the cultures were incubated for 12–24 h at 37 °C and 5% CO₂ in order to achieve cell attachment to the coverslip. Then, the cells were treated with the test compounds (1 µM, 10 µM) and incubated for 1 h, 3 h, 6 h, or 9 h at 37 °C and 5% CO₂. The coverslips with the attached cells were transferred into another 12-well plate containing PBS. After washing with PBS for three times the PBS was removed from the wells and the HeLa cells were fixed by treatment with ice-cold methanol for 1 h at 4 °C. The methanol was removed and the cells were washed again for three times with PBS. Primary antibody

(mouse anti α -tubulin monoclonal IgG (TAT), 1 μ g/mL in PBS) was added to the cells and incubated at room temperature in a humid chamber in the dark for 1 h. The coverslips were washed with PBS for three times and secondary antibody (Anti-Mouse IgG ATTO 550, Sigma, 1.5 μ g/mL in PBS) was added to the cells and incubated in a humid chamber in the dark at room temperature for 1 h. After washing with PBS for three times (5 min) and removal of the PBS the cells were embedded with Vectashield Mounting Medium (Vector Laboratories) containing DAPI (1.5 μ g/mL) and analyzed via fluorescence microscopy.

Similarly, trypanosome cells (3×10^6 cells/mL) were placed into 12-well plates containing supplemented HMI-9 medium (1 mL) at 37 °C. Test compounds (0.1 μ M, 0.5 μ M, 1 μ M, 10 μ M) were added and the cells were incubated for 0.5 h, 1 h, 3 h, and 6 h at 37 °C and 5% CO₂. After centrifugation at 3341 \times g for 1 min, the cell pellet was resuspended in 500 μ L PEME medium (0.1 M PIPES, 2 mM EGTA, 1 mM MgSO₄, 0.1 mM EDTA, pH 6.9) and washed with PEME for three times. The cells (150 μ L, in PEME medium) were placed on poly-lysine-coated glass microscope slides and incubated to attach to the slide in a humid chamber for 10 min at room temperature. After careful washing with PEME and extraction with ice-cold 1% NP40 in PEME for 5 min the cells were briefly washed in PEME and then fixed in ice-cold methanol for 1 h followed by treatment of the fixed cells with PBS for 5 min. Staining with the primary and secondary antibodies and embedding as well as fluorescence analyses were carried out analogously to the HeLa cell protocol described above.

4.8. Isolation of *Entamoeba histolytica* and in vitro susceptibility

Entamoeba histolytica samples were taken from patients of the Ibrahim Malik Hospital (Khartoum, Sudan). Positive samples were identified by wet mount preparation. The positive samples were transported to the laboratory in nutrient broth medium. Trophozoites of the parasites were maintained in RPMI 1640 medium containing 5% bovine serum at 37 \pm 1 °C. The trophozoites were maintained for the assays and were employed in the log phase of growth. A stock solution of **2c** in DMSO (1 mg/mL) was prepared and diluted to final concentrations of 100, 50 and 25 μ g/mL, respectively, in microtiter well plates (total volume of 100 μ L in each well) with distilled water and culture medium containing the trophozoites. Metronidazole (200 μ g/mL) was applied as a positive control, whereas untreated cells were used as negative controls (i.e., culture medium plus trophozoites). For cell counting, the samples were mixed with Trypan blue in equal volume. The final number of parasites was determined with a hemocytometer for three times after 24 h, 48 h, and 72 h. The mortality (in %) of parasites was calculated according to the following formula:

$$\text{Mortality (\%)} = \frac{[(\text{neg. control} - \text{tested sample})/\text{neg. control}] \times 100}{1}$$

Theoretically, no motile parasites are observed at 100% inhibition.

Statistical analysis for all assay results was done using Microsoft Excel program. Student *t*-test was applied to determine significant differences between controls and test compounds (*P* < 0.05).

Acknowledgements

B.B. is grateful to the Maharashtra Cosmopolitan Education Society (Mr. P.A. Inamdar and Mrs. Abeda Inamdar) and Dr. E.M. Khan of the Abeda Inamdar Senior College, Pune, for the provision of a scholarship.

Appendix A. Supplementary data

Supplementary data related to this article can be found at <http://dx.doi.org/10.1016/j.ejmech.2016.11.043>.

References

- [1] R.E. Talcott, M.T. Smith, D.D. Giannini, Inhibition of microsomal lipid peroxidation by naphthoquinones: structure-activity relationships and possible mechanisms of action, *Arch. Biochem. Biophys.* 241 (1985) 88–94.
- [2] S. Reese, A. Vidyasagar, L. Jacobson, Z. Acun, S. Esnault, D. Hullett, J.S. Malter, A. Djamali, The Pin 1 inhibitor juglone attenuates kidney fibrogenesis via Pin 1-independent mechanisms in the unilateral ureteral occlusion model, *Fibrog. Tissue Rep.* 3 (2010) 1.
- [3] A.S. Borade, B.N. Kale, R.V. Shete, A phytopharmacological review on *Lawsonia inermis* (Linn.), *Int. J. Pharm. Life Sci.* 2 (2011) 536–541.
- [4] R. Pradhan, P. Dandawate, A. Vyas, S. Padhye, B. Biersack, R. Schobert, A. Ahmad, F.H. Sarkar, From body art to anticancer activities: perspectives on medicinal properties of Henna, *Curr. Drug Targets* 13 (2012) 1777–1798.
- [5] A.V. Pinto, S.L. de Castro, The trypanocidal activity of naphthoquinones: a review, *Molecules* 14 (2009) 4570–4590.
- [6] K.M. Nadkarni, *Indian Plants and Drugs*, Asiatic Publishing House, Delhi, 2000.
- [7] K.S. Ahluwalia, *The British Pharmaceutical Codex Plants and Their Indian Substitutes*, Ministry of Health, Government of India, New Delhi, 1967.
- [8] M. d'Arcy Doherty, A. Rodgers, G.M. Cohen, Mechanisms of toxicity of 2- and 5-hydroxy-1,4-naphthoquinone; absence of a role for redox cycling in the toxicity of 2-hydroxy-1,4-naphthoquinone to isolated hepatocytes, *J. Appl. Toxicol.* 7 (1987) 123–129.
- [9] K. Öllinger, A. Brunmark, Effect of hydroxyl substituent position on 1,4-naphthoquinone toxicity to rat hepatocytes, *J. Biol. Chem.* 266 (1991) 21496–21503.
- [10] H. Babich, A. Stern, *In vitro* cytotoxicities of 1,4-naphthoquinone and hydroxylated 1,4-naphthoquinones to replicating cells, *J. Appl. Toxicol.* 13 (1993) 353–358.
- [11] S.-H. Wang, C.-Y. Lo, Z.-H. Gwo, H.-J. Lin, L.-G. Chen, C.-D. Kuo, J.-Y. Wu, Synthesis and biological evaluation of lipophilic 1,4-naphthoquinone derivatives against human cancer cell lines, *Molecules* 20 (2015) 11994–12015.
- [12] S. Oramas-Royo, C. Torrejón, I. Cuadrado, R. Hernández-Molina, S. Hortelano, A. Estévez-Braun, B. de las Heras, Synthesis and cytotoxic activity of metallic complexes of lawsone, *Bioorg. Med. Chem.* 21 (2013) 2471–2477.
- [13] A. Baramee, A. Coppin, M. Mortuaire, L. Pelinski, S. Tomavo, J. Brocard, Synthesis and *in vitro* activities of ferrocenic aminohydroxynaphthoquinones against *Toxoplasma gondii* and *Plasmodium falciparum*, *Bioorg. Med. Chem.* 14 (2006) 1294–1302.
- [14] A.V. Pinto, C.N. Pinto, M.C.F.R. Pinto, R.S. Rita, C.A. Pezzella, S.L. de Castro, Trypanocidal activity of synthetic heterocyclic derivatives of active quinones from *Tabebuia* sp. *Arzneimittelforsch* 47 (1997) 74–79.
- [15] R.S.F. Silva, E.M. Costa, U.L.T. Trindade, D.V. Teixeira, M.C.F.R. Pinto, G.L. Santos, V.R.S. Malta, C.A. de Simone, A.V. Pinto, S.L. de Castro, Synthesis of naphthofuranquinones with activity against *Trypanosoma cruzi*, *Eur. J. Med. Chem.* 41 (2006) 526–530.
- [16] M.L. Bolognesi, F. Lizzi, R. Perozzo, R. Brun, A. Cavalli, Synthesis of a small library of 2-phenoxy-1,4-naphthoquinone and 2-phenoxy-1,4-antraquinone derivatives bearing anti-trypanosomal and anti-leishmanial activity, *Bioorg. Med. Chem. Lett.* 18 (2008) 2272–2276.
- [17] A.O. da Silva, R. da Silva Lopes, R.V. de Lima, C.S.S. Tozatti, M.R. Marques, S. de Albuquerque, A. Beatriz, D.P. de Lima, Synthesis and biological activity against *Trypanosoma cruzi* of substituted 1,4-naphthoquinones, *Eur. J. Med. Chem.* 60 (2013) 51–56.
- [18] A. Sharma, I.O. Santos, P. Gaur, V.F. Ferreira, C.R.S. Garcia, D.R. da Rocha, Addition of thiols to *o*-quinone methide: new 2-hydroxy-3-phenylsulfanylmethyl[1,4]naphthoquinones and their activity against the human malaria parasite *Plasmodium falciparum* (3D7), *Eur. J. Med. Chem.* 59 (2013) 48–53.
- [19] A.P. Neves, G.B. da Silva, M.D. Vargas, C.B. Pinheiro, L.D.C. Visentin, J.D.B.M. Filho, A.J. Araujo, L.V. Costa-Lotufo, C. Pessoa, M.O. de Moraes, Novel platinum(II) complexes of 3-(aminomethyl)naphthoquinone Mannich bases: synthesis, crystal structure and cytotoxic activities, *Dalton Trans.* 39 (2010) 10203–10216.
- [20] G.B. da Silva, A.P. Neves, M.D. Vargas, J.D.B. Marinho-Filho, L.V. Costa-Lotufo, New insights into 3-(aminomethyl)naphthoquinones: evaluation of cytotoxicity, electrochemical behaviour and search for structure-activity correlation, *Bioorg. Med. Chem. Lett.* 26 (2016) 3537–3542.
- [21] A. Ahmad, K. Mahal, S. Padhye, F.H. Sarkar, R. Schobert, B. Biersack, New ferrocene modified lawsone Mannich bases with anti-proliferative activity against tumor cells, *J. Saudi Chem. Soc.* (2016), <http://dx.doi.org/10.1016/j.jscs.2016.03.005>.
- [22] W. Paengsri, A. Baramee, Synthesis and evaluation of anti-tuberculosis and anti-cancer activities of hydroxynaphthoquinone derivatives, *Chiang Mai J. Sci.* 40 (2013) 70–76.
- [23] S.V. Malhotra, V. Kumar, C. Velez, B. Zayas, Imidazolium-derived ionic salts induce inhibition of cancerous cell growth through apoptosis, *Med. Chem. Commun.* 5 (2014) 1404–1409.

- [24] F. Prati, C. Bergamini, M.T. Molina, F. Falchi, A. Cavalli, M. Kaiser, R. Brun, R. Fato, M.L. Bolognesi, 2-Phenoxy-1,4-naphthoquinones: from a multitarget antitrypanosomal to a potential antitumor profile, *J. Med. Chem.* 58 (2015) 6422–6434.
- [25] F. Prati, E. Uliassi, M.L. Bolognesi, Two diseases, one approach: multitarget drug discovery in Alzheimer's and neglected tropical diseases, *Med. Chem. Commun.* 5 (2014) 853–861.
- [26] S.B.B.B. Bahia, W.J. Reis, G.A.M. Jardim, F.T. Souto, C.A. de Simone, C.C. Gatto, R.F.S. Menna-Barreto, S.L. de Castro, B.C. Cavalcanti, C. Pessoa, M.H. Araujo, E.N. da Silva Júnior, Molecular hybridization as a powerful tool towards multitarget quinoidal systems: synthesis, trypanocidal and antitumor activities of naphthoquinone-based 5-iodo-1,4-disubstituted-, 1,4- and 1,5-disubstituted-1,2,3-triazoles, *Med. Chem. Commun.* 7 (2016) 1555–1563.
- [27] A.P. Neves, M.D. Vargas, C.A.T. Soto, J.M. Ramos, L.D.C. Visentin, C.B. Pinheiro, A.S. Mangrich, E.I.P. de Rezende, Novel zinc(II) and copper(II) complexes of a Mannich base derived from lawsone: synthesis, single crystal X-ray analysis, *ab initio* density functional theory calculations and vibrational analysis, *Spectrochim. Acta A* 94 (2012) 152–163.
- [28] E.A. Hillard, F.C. de Abreu, D.C.M. Ferreira, G. Jaouen, M.O.F. Goulart, C. Amatore, Electrochemical parameters and techniques in drug development, with an emphasis on quinones and related compounds, *Chem. Commun.* (2008) 2612–2628.
- [29] A.J. Araújo, A.A. de Souza, E.N. da Silva Júnior, J.D.B. Marinho-Filho, M.A.B.F. de Moura, D.D. Rocha, M.C. Vasconcelos, C.O. Costa, C. Pessoa, M.O. de Moraes, V.F. Ferreira, F.C. de Abreu, A.V. Pinto, R.C. Montenegro, L.V. Costa-Lotufo, M.O.F. Goulart, Growth inhibitory effects of 3'-nitro-3-phenylamino nor-beta-lapachone against HL-60: a redox-dependent mechanism, *Toxicol. In Vitro* 26 (2012) 585–594.
- [30] O. Ramirez, L.B. Motta-Mena, A. Cordova, K.M. Garza, A small library of synthetic di-substituted 1,4-naphthoquinones induces ROS-mediated cell death in murine fibroblasts, *PLoS One* 9 (2014) e0106828.
- [31] L.-O. Klotz, X. Hou, C. Jacob, 1,4-Naphthoquinones: from oxidative damage to cellular and inter-cellular signaling, *Molecules* 19 (2014) 14902–14918.
- [32] T.P.C. Dorlo, M. Balasegaram, J.H. Beijnen, P.J. de Vries, Miltefosine: a review of its pharmacology and therapeutic efficacy in the treatment of leishmaniasis, *J. Antimicrob. Chemother.* 67 (2012) 2576–2597.
- [33] A. Kostadinova, B. Nikolova, P. Handjiiska, M.R. Berger, I. Tsoneva, Combined effect of electroporation and miltefosine on keratinocyte cell line HaCaT, *Rom. Rep. Phys.* 67 (2015) 995–1003.
- [34] T. Mosmann, Rapid colorimetric assay for cellular growth and survival: application to proliferation and cytotoxic assays, *J. Immunol. Methods* 65 (1983) 55–63.
- [35] J.K. Muenzner, B. Biersack, A. Albrecht, T. Rehm, U. Lacher, W. Milius, A. Casini, J.-J. Zhang, I. Ott, V. Brabec, O. Stuchlikova, I.C. Andronache, L. Kaps, D. Schuppan, R. Schobert, Ferrocenyl-coupled *N*-heterocyclic carbene complexes of gold(I): a successful approach to multinuclear anticancer drugs, *Chem. Eur. J.* (2016), <http://dx.doi.org/10.1002/chem.201604246>.
- [36] R.S. Twigg, Oxidation-reduction aspects of resazurin, *Nature* 155 (1945) 401–402.
- [37] R.D. Fields, M.V. Lancaster, Dual-attribute continuous monitoring of cell proliferation/cytotoxicity, *Am. Biotechnol. Lab.* 11 (1993) 48–50.
- [38] S.A. Ahmed, R.M. Gogal Jr., J.E. Walsh, A new rapid and simple non-radioactive assay to monitor and determine the proliferation of lymphocytes, *J. Immunol. Methods* 170 (1994) 211–224.
- [39] S. Al-Nasiry, N. Geusens, M. Hanssens, C. Luyten, R. Pijnenborg, The use of Alamar Blue assay for quantitative analysis of viability, migration and invasion of choriocarcinoma cells, *Hum. Rep.* 22 (2007) 1304–1309.